Indian Journal of Chemical Technology
Vol. 23, September 2016, pp. 345-352

Adsorption and corrosion inhibition behaviour of acid red on AISI 4130 alloy steel in HCl solution

I Danaee*, Z Moallem, H Eskandari & S Nikmanesh

Abadan Faculty of Petroleum Engineering, Petroleum University of Technology, Abadan, Iran
E-mail: danaee@put.ac.ir

Received 8 April 2014; accepted 6 May 2016

The inhibition behaviour of 2-(N,N-Dimethyl-4-aminophenyl)azobenzenecarboxylic acid (acid red) on the corrosion resistance of AISI 4130 steel in 1 M HCl solution has been studied by potentiodynamic polarization (Tafel), electrochemical impedance spectroscopy (EIS) and scanning electron microscopy (SEM). Polarization studies indicate that the inhibition efficiency increases with the increase in inhibitor concentration and inhibitor retard both the cathodic and anodic reactions so classified as mixed type inhibitors. EIS data has been analyzed to equivalent circuit model and show that as the inhibitor concentration increased the charge transfer resistance of steel increased whilst double layer capacitance decreased. The effect of temperature on the corrosion behavior of steel in HCl with the addition of the inhibitor was studied in the temperature range from 25-65°C. The experimentally obtained adsorption isotherms follow the Langmuir equation. Activation parameters and thermodynamic adsorption parameters of the corrosion process such as $\boldsymbol{E}_a$, $\Delta\boldsymbol{H}$, $\Delta\boldsymbol{S}$, $\boldsymbol{K}_{ads}$ and $\Delta\boldsymbol{G}°_{ads}$ are calculated at different temperatures and using the adsorption isotherm. The morphology of steel surface after its exposure to HCl solution in the absence and presence of inhibitor has been examined by SEM images.

Keywords: AISI 4130 steel, Corrosion inhibitor, Acid red, Potentiodynamic polarization, Adsorption, Langmuir, SEM

Acid solutions are generally used for the removal of rust and scale in some industrial processes. Among these, hydrochloric acid is one of the most widely used agents in the process of acid pickling. Generally, hydrochloric acid solutions are used for pickling, chemical and electrochemical etching of some metals and alloys[1].

Due to the exposure of steel to corrosive environments, they are susceptible to different types of corrosion mechanisms. One of the methods used to reduce the rate of corrosion is addition of inhibitors. Many studies have been carried out to find suitable compounds to be used as corrosion inhibitors for steel in hydrochloric acid solutions[2-8].

Organic inhibitors adsorb on the metal surface and suppress metal dissolution and reduction reactions. In most cases, it appears that adsorbed inhibitors affect both the anodic and cathodic process although in many cases the effect is unequal[9]. It was shown that organic compounds containing heteroatoms such as nitrogen, sulphur, oxygen and phosphorous are capable of forming coordinate covalent bond with metal owing to their free electron pairs and thus acting as inhibitor. π Electrons in triple or conjugated double bonds also exhibit good inhibitive properties[10-12]. Among various organic inhibitors, organic dyes whose molecules meet certain desirable characteristics as potential corrosion inhibitors have been attracted more attention[13-16]. Recently, it was reported that the different organic dyes shown inhibition behavior on mild steel in 1 M HClsolution[15-16].

The 4130 steel is widely used in petroleum and gas industry. This steel is a low alloy steel containing molybdenum and chromium as strengthening agents and is also widely used in structural applications such as aircraft engine mounts or welded tubing and piping applications[17,18]. The present work is devoted to investigate the corrosion behavior of 4130 steel in hydrochloric acid solutions over a certain concentration range of acid red as corrosion inhibitor. To prove the effectiveness of this compound, potentiodynamic polarization measurements, electrochemical impedance spectroscopy, and chrono-amperometry were used.

Experimental Section

Materials

Materials used in this work were from Merck (Darmstadt, Germany) products of analytical grade and were used without further purifications. The exposed surface area of each electrode is equal to 1 cm^2. These specimens were used as working

electrode in electrochemical measurements and the exposed areas of the electrodes were mechanically abraded with 220, 400, 600, 800, 1000 and 1200 grades of emery paper, degreased with acetone and rinsed by distilled water before each electrochemical experiment.

The chemical composition of the steel 4130 samples (wt%) was distinguished by Spectrolab quantometer (C: 0.28, Si: 0.13, Mn: 0.69, P: 0.02, S:0.021, Cr: 1, Ni: 0.23, Mo: 0.16, Cu: 0.22, V: 0.002, W: 0.008, Sn: 0.02, Pb: 0.002, As: 0.009, Sb: 0.005 w%, Fe: Base). The concentration range of inhibitor employed was varied from 40 to 100 ppm. Figure 1 shows the chemical structure of acid red.

Methods

Electrochemical measurements were carried out in a conventional three-electrode system. A saturated Ag/AgCl and a platinum sheet were used as the reference electrode and the counter electrode, respectively. Before each experiment, the working electrode was immersed in the test cell for 30 min until reaching steady state condition. The electrochemical measurements were carried out using computer controlled Auto Lab potentiostat/ galvanostat (PGSTAT 302 N). Polarization curves were recorded at constant sweep rate of 1 mV s^{-1} from -600 mV to 0 mV with respect to reference electrodes. All tests were carried out at constant temperature by controlling the cell temperature using a water bath. The electrochemical tests were conducted at 25, 45 and 65°C temperatures.

Corrosion current $\boldsymbol{I_{corr}}$ was calculated from Tafel extrapolation methods. The measurements were repeated three times for each condition and the average values were presented. Electrochemical impedance spectroscopy (EIS) measurements were carried out in frequency range from 100 kHz to 10 mHz with amplitude of 10 mV peak-to-peak using AC signals at open circuit potential. Fitting of experimental impedance spectroscopy data to the proposed equivalent circuit was done by means of homewritten least square software based on the Marquardt method for the optimization of functions and Macdonald weighting for the real and imaginary parts of the impedance[19,20].

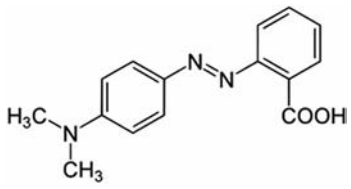

Fig. 1 — Chemical structure of acid red.

Result and Discussion

Potentiodynamic polarization measurement

Figure 2 shows the anodic and cathodic polarization plots of steel in 1 MHCl in the absence and presence of acid red in different concentrations at 25°C. Table 1 gives the electrochemical corrosion parameters such as corrosion potential ($\boldsymbol{E_{corr}}$), corrosion current density ($\boldsymbol{I_{corr}}$), cathodic and anodic

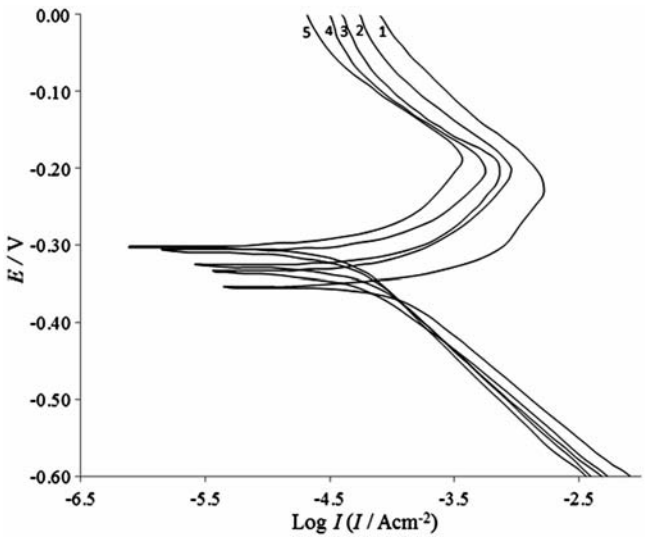

Fig. 2 — Anodic and cathodic polarization curves for steel in 1 M HCl without and withdifferent concentration of acid red at 25°C: (1) Blank, (2) 40, (3) 60, (4) 80, (5) 100 ppm.

Table 1 — Potentiodynamic polarization parameters for the corrosion of steel in 1 M HCl solution in absence and presence of different concentrations of acid red at 25°C.

Concentration ppm	$I_{corr}\times10^6$ A cm^{-2}	β_a mV dec^{-1}	β_c mV dec^{-1}	$-E_{corr}$ mV	R_p Ω cm^2	CR mpy	θ	IE %
0	104	73.1	89.1	353	166.6	48.02	…..	…..
40	39.2	75.7	91.3	339	458.4	17.98	0.62	62
60	33.7	73.4	98.2	335	541.2	15.46	0.68	68
80	30.5	74.5	112	323	635.9	13.99	0.71	71
100	27.5	81.5	115	302	753.1	12.62	0.73	73

Tafel slopes (β_c, β_a), the degree of surface coverage (θ), inhibition efficiency (***IE***%) and polarization resistance (***R_p***). The degree of surface coverage and inhibition efficiency for different concentrations of inhibitor were calculated using the following equations[21,22]:

$$= (1 - \frac{\boldsymbol{I}}{\boldsymbol{I}_0}) \quad ...(1)$$

$$\boldsymbol{IE}\% = (\times 100) \quad ...(2)$$

where ***I_0*** and ***I*** are the corrosion current densities for steel in uninhibited and inhibited acid solution, respectively.

Figure 2 shows that the decrease in corrosion rate is associated with a shift of both cathodic and anodic branches of the polarization curves towards lower current densities. These results suggest that this compound acts as mixed-type inhibitor[23-27]. In each case the whole curves are shifted towards lower current density values compared to that of the blank solution. Also it can be seen that the corrosion rate decreased and inhibition efficiency (***IE*** %) increased by increasing inhibitor concentration.

The corrosion current density is related to the polarization resistance by the Stern-Geary equation:

$$\boldsymbol{I}_{corr} = \frac{10^6 \times \boldsymbol{B}}{\boldsymbol{R}_p} \quad ...(3)$$

The Stern-Geary coefficient B is related to the anodic, β_a, and cathodic, β_c, Tafel slopes as below [28].

$$\boldsymbol{B} = \frac{{}_a \times {}_c}{2.303 ({}_a + {}_c)} \quad ...(4)$$

By increasing the inhibitor concentration, the polarization resistance increases in the presence of compound, indicating adsorption of the inhibitor on the metal surface to block the active sites efficiently and inhibit corrosion[29].

Electrochemical impedance spectroscopy

The corrosion of steel in 1 M HCl solutions in the absence and presence of acid red was investigated by electrochemical impedance spectroscopy. Nyquist plots obtained in the absence and presence of various concentrations of inhibitor are given in Fig. 3. These diagrams have similar shape throughout all tested concentrations, indicating that almost no change in the corrosion mechanism occurs due to the inhibitor addition. Nyquist plots show a depressed capacitive loop which arises from the time constant of the electrical double layer and charge transfer resistance, indicating that the corrosion process was mainly charge transfer controlled[30]. The diameter of Nyquist plots increases with increasing the inhibitor concentration. This suggested that the formed inhibitive film was strengthened by addition of inhibitors. The impedance spectra for different Nyquist plots were analyzed by fitting the experimental data to a simple equivalent circuit model[31]. The equivalent circuit compatible with the Nyquist diagram recorded in the presence of inhibitors was depicted in Fig. 4. The simplest approach requires the theoretical transfer function ***Z*** (ω) to be represented by a parallel combination of a resistance ***R_ct*** and a capacitance ***C***, both in series with another resistance ***R_s***[32]:

$$\boldsymbol{Z}( ) = \boldsymbol{R}_s + \frac{1}{1/\boldsymbol{R}_{ct} + \boldsymbol{i} \ \boldsymbol{C}} \quad ...(5)$$

ω is the frequency in rad/s, $\omega = 2\pi \boldsymbol{f}$ and ***f*** is frequency in Hz. To obtain a satisfactory impedance simulation of steel, it is necessary to replace the capacitor (***C***) with a constant phase element (***CPE***) ***Q*** in the equivalent circuit. The most widely accepted

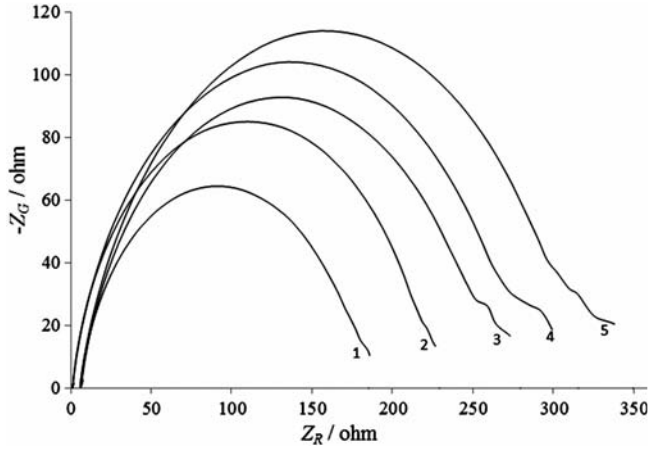

Fig. 3 — Nyquist plots for steel in 1 M HCl without and withdifferent concentration of acid red at 25°C: (1) Blank, (2) 40, (3) 60, (4) 80, (5) 100 ppm.

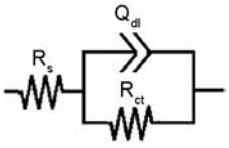

Fig. 4 — Equivalent circuits compatible with the experimental impedance data for corrosion of steel electrode in different inhibitors concentrations.

explanation for the presence of ***CPE*** behavior and depressed semicircles on solid electrodes is microscopic roughness, causing an inhomogeneous distribution in the solution resistance as well as in the double-layer capacitance[33]. Constant phase element Q_{dl}, R_s and R_{ct} can be corresponded to double layer capacitance, solution resistance, and charge transfer resistance respectively. To corroborate the equivalent circuit, the experimental data are fitted to equivalent circuit and the circuit elements are obtained. Table 2 illustrates the equivalent circuit parameters for the impedance spectra of corrosion of steel in 1 M HCl solution. The results demonstrate that the presence of inhibitor enhance the value of R_{ct} obtained in the pure medium while that of Q_{dl} is reduced[34]. The decrease in Q_{dl} values was caused by adsorption of inhibitor indicating that the exposed area decreased. On the other hand, a decrease in Q_{dl}, which can result from a decrease in local dielectric constant and/or an increase in the thickness of the electrical double layer, suggests that inhibitor act by adsorption at the metal-solution interface.

As the Q_{dl} exponent (n) is a measure of the surface heterogeneity, values of n indicates that the steel surface becomes more and more homogeneous as the concentration of inhibitor increases as a result of its adsorption on the steel surface and corrosion inhibition. The increase in values of R_{ct} and the decrease in values of Q_{dl} with increasing the concentration also indicate that acid red acts as primary interface inhibitor and the charge transfer controls the corrosion of steel under the open circuit conditions.

Effect of temperature

The effect of temperature on the inhibited metal corrosion reaction is very complex, because many changes occur on the metal surface such as rapid desorption of inhibitor. The change of the corrosion rate with the temperature was studied in the absence and presence of acid red in 1 M HCl. For this purpose, polarization was performed at different temperatures from 25 to 65°C in absence and presence of different concentrations of inhibitors (Fig. 5). For 45°C and 65°C the electrochemical parameters were extracted and summarized in Tables 3 and 4. It is obvious that the values of I_{corr} increases by increasing in temperature in both solutions but the efficiency values increase. The figures show that raising the temperature leads to a higher corrosion rate. According to the Arrhenius equation, the apparent activation energy (E_a) of metal corrosion in both media (Blank and inhibited) can be calculated from the following equation[35]:

$$I_{corr} = A\exp(-\frac{E_a}{RT}) \quad ...(6)$$

where E_a represents the apparent activation energy, R the gas constant, A the pre-exponential factor, T

Table 2 — Impedance data for steel in 1 M HCl solution without and with different concentrations of acid red at 25°C.

Concentration ppm	R_s / Ω	R_{ct} / Ω	$Q_{dl}\times10^3$ / F	n
0	6.2	174	0.51	0.84
40	1.3	218	0.42	0.83
60	6.6	254	0.37	0.83
80	1.4	278	0.32	0.86
100	5.9	313	0.31	0.87

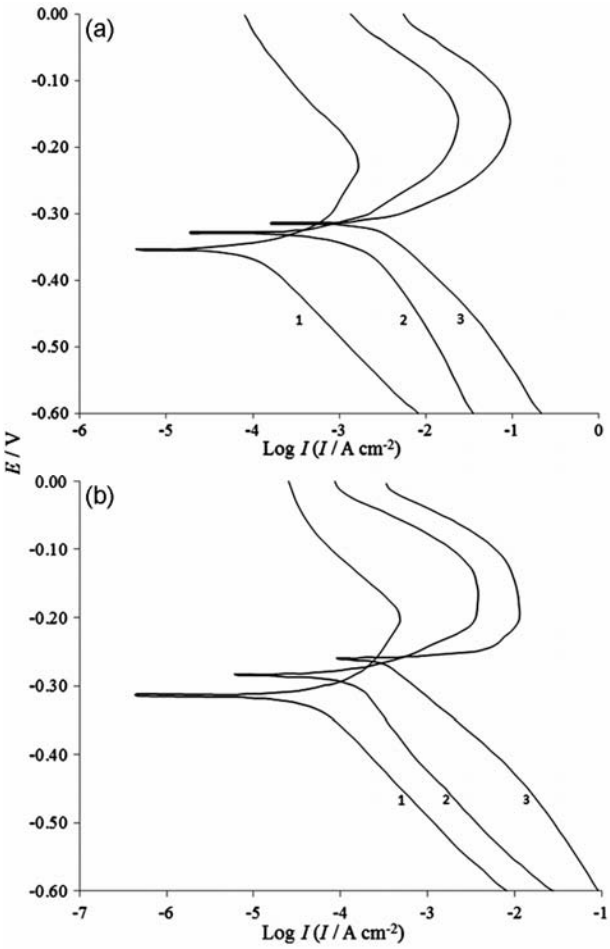

Fig. 5 — Anodic and cathodic polarization curves for steel in 1M HCl(a) without inhibitor and (b) with 100 ppm of acid red at different temperatures: (1) 25°C, (2) 45°C, (3) 65°C.

Table 3 — Electrochemical parameters for the corrosion of steel in 1 M HCl solution in absence and presence of different concentrations of acid red at 45°C

Concentration ppm	$I_{corr}\times10^6$ A cm^{-2}	β_a mV dec^{-1}	β_c mV dec^{-1}	$-E_{corr}$ mV	R_p Ω cm^2	CR mpy	θ	IE %
0	539	78.4	88.2	326	33.43	247.4	…..	…..
40	221	76.5	129	317	94.27	101.5	0.59	59
60	143	75.8	128	301	144.9	65.44	0.73	73
80	102	84.6	115	298	207.2	46.89	0.81	81
100	80.2	83.2	109	292	255.5	36.80	0.85	85

Table 4 — Electrochemical parameters for the corrosion of steel in 1 M HCl solution in absence and presence of different concentrations of acid red at 65 °C.

Concentration ppm	$I_{corr}\times10^6$ A cm^{-2}	β_a mV dec^{-1}	β_c mV dec^{-1}	$-E_{corr}$ mV	R_p Ω cm^2	CR mpy	θ	IE %
0	2830	83.9	179	316	8.765	1298.81	…..	…..
40	982.2	82.1	148	268	23.31	450.79	0.65	65
60	672.3	85.2	151	267	35.22	308.50	0.76	76
80	502.6	84.8	168	259	48.69	230.69	0.82	82
100	388.1	83.2	183	252	64.01	178.16	0.86	86

the absolute temperature. The logarithm of I_{corr} against the reciprocal of temperature (T^{-1}) is straight line in the absence and presence of acid red. The activation energy E_a is calculated from the slope of the straight lines (- E_a/R) in different inhibitor concentrations. Table 5 shows that values of E_a in 1 M HCl containing inhibitors are lower than that in uninhibited solution indicating that the inhibitory action of inhibitor for steel corrosion in HCl media occurs via chemisorption[36]. Furthermore; decrease in A reduces the corrosion rate of the carbon steel. So, the corrosion rate of steel decreased with increasing the inhibitor concentration[37].

It was reported that inhibitors for which E_a is smaller in the presence of inhibitor than in the absence of that in the solution undergo chemisorption[38]. The chemical adsorption is due to formation of coordinated bond between the d-orbital of iron and inhibitor molecules on the surface of steel through lone pair of electron of N, S and O atoms[39]. Szauer and Brand explained that the decrease in activation energy can be referred to a considerable increase in the adsorption of the inhibitor on the steel surface with increase in temperature. As more adsorption of inhibitor molecules occurs, desorption decreases because these two opposite processes are in equilibrium. More adsorption of inhibitor molecules at higher temperatures makes the lower surface area of steel exposes in contact with acid environment, resulting increased inhibition efficiency with increase in temperature [40].

Table 5 — Activation parameters of the dissolution of steel in 1 M HCl solution in the absence and presence of acid red.

Concentration ppm	E_a kJ mol^{-1}	A A cm^{-2}	ΔH_a kJ mol^{-1}	ΔS_a J mol^{-1}	E_a - ΔH_a kJ mol^{-1}
0	69.10	1.34×10^8	66.46	-98.19	2.6
40	67.49	2.62×10^7	64.86	-111.7	2.6
60	62.73	3.29×10^6	60.09	-129.0	2.6
80	58.72	5.91×10^5	56.08	-143.3	2.6
100	55.47	1.44×10^5	52.83	-155.0	2.6

Enthalpy and entropy of activation (ΔH_a, ΔS_a) were calculated from the transition state theory [41,42]:

$$I_{corr} = \frac{RT}{Nh}\exp(-\frac{\Delta H_a}{RT})\exp(\frac{\Delta S_a}{R}) \quad ...(7)$$

where I_{corr} is the corrosion rate, h is the Planck's constant, N is the Avogadro's number, R is the gas constant, T is the absolute temperature, ΔH_a is the enthalpy and ΔS_a is the entropy of activation. A plot of $\ln(I_{corr}\ T^{-1})$ versus T^{-1} give straight lines for steel dissolution in HCl solution in the absence and presence of different concentrations of inhibitors. Straight lines are obtained with a slope of $-\Delta H_a/R$ and an intercept of $\ln(R/Nh) + \Delta S_a/R$.

Investigation of these data shows that the ΔH_a for dissolution reaction of steel in 1 M HCl in the presence of inhibitors are lower than that of the absence of inhibitor. The positive values of ΔH_a mean that the dissolution reaction is an endothermic process in HCl solution[43-45]. Large and negative values of

entropies show that the activated complex in the rate determining step represents an association rather than a dissociation step, meaning that a decrease in disordering takes place on going from reactants to the activated complex[46].

Adsorption isotherm

Basic thermodynamic information on interaction between metal surface and inhibitor molecules can be provided by adsorption isotherms that are employed for thermodynamic calculations of inhibitor adsorption. There are different adsorption isotherms such as Langmuir, Temkin, Ei-Away, Bockris–Swinkels, Flory–Huggins and Frumkin, etc[47,48]. In this study, different adsorption isotherms were checked for determining the best adsorption isotherms for inhibitor. For this inhibitor, in different temperatures and concentrations the plots were sketched. Among these plots one of them with highest regression is selected and an adsorption isotherm is determined. It was found that the experimental data obtained from polarization readings could be fitted by Langmuir's adsorption isotherm. Inhibitive action of acid red could be due to the adsorption of its molecules on the steel surface making a barrier for charge and mass transfer between the metal and the environment. As the concentration of inhibitor was increased, the fraction of steel surface covered by the adsorbed molecules (θ) increases leading to higher inhibition efficiency. According to isotherm, the surface coverage is related to inhibitor concentration by:

$$\frac{\theta}{1-\theta} = \boldsymbol{K}_{\boldsymbol{ads}}\boldsymbol{C} \qquad ...(8)$$

where $\boldsymbol{K}_{\text{ads}}$ is constant of adsorption[48,49]. The plots of $\theta/(1-\theta)$ versus $\boldsymbol{C}$ in different temperature and concentration of inhibitor show straight lines. This isotherm assumes that the adsorbed molecules occupy only one site, and the inhibitor forms a mono (-molecule) layer on the steel surface and there are no interactions with other adsorbed species.

The most important thermodynamic adsorption parameters are the free energy of adsorption ($\Delta\boldsymbol{G}^{\circ}_{\boldsymbol{ads}}$), the heat of adsorption ($\Delta\boldsymbol{H}^{\circ}_{\boldsymbol{ads}}$) and the entropy of adsorption ($\Delta\boldsymbol{S}^{\circ}_{\boldsymbol{ads}}$). The adsorption constant, $\boldsymbol{K}_{\text{ads}}$, is related to the standard free energy of adsorption, $\Delta\boldsymbol{G}^{\circ}_{\boldsymbol{ads}}$, with the following equation:

$$\boldsymbol{K}_{\boldsymbol{ads}} = \frac{1}{55.5}\exp\left(-\frac{\Delta\boldsymbol{G}_{\boldsymbol{ads}}}{\boldsymbol{RT}}\right) \qquad ...(9)$$

where 55.5 is the water concentration of solution in mL/L[46]. The standard free energy of adsorption ($\Delta\boldsymbol{G}^{\circ}_{\boldsymbol{ads}}$) values were calculated and given in Table 6. The high value of $\boldsymbol{K}_{\text{ads}}$ and negative values of $\Delta\boldsymbol{G}^{\circ}_{\boldsymbol{ads}}$ indicate the stability of the adsorbed layer on the steel surface and the spontaneous adsorption of inhibitors[50].

Usually, the magnitude of standard free energy of adsorption around −20 kJ mol^{-1} or less negative is considered for electrostatic interactions between inhibitor molecules and charged metal surface (i.e., physisorption). The magnitude of $\Delta\boldsymbol{G}^{\circ}$ near −40 kJ mol^{-1} or more negative is usually assumed for charge sharing or transferring from organic molecules to the metal surface to form a coordinate type of metal bond (i.e., chemisorption)[51]. In this work $\Delta\boldsymbol{G}^{\circ}_{\boldsymbol{ads}}$ is a negative value and near −40 kJ mol^{-1} so the adsorption process is chemisorption.

The enthalpy and entropy of adsorption ($\Delta\boldsymbol{H}^{\circ}_{\boldsymbol{ads}}$ and $\Delta\boldsymbol{S}^{\circ}_{\boldsymbol{ads}}$) can be calculated using the following equation[47]:

$$\Delta\boldsymbol{G}_{\boldsymbol{ads}} = \Delta\boldsymbol{H}_{\boldsymbol{ads}} - \boldsymbol{T}\Delta\boldsymbol{S}_{\boldsymbol{ads}} \qquad ...(10)$$

where $\Delta\boldsymbol{H}^{\circ}_{\boldsymbol{ads}}$ and $\Delta\boldsymbol{S}^{\circ}_{\boldsymbol{ads}}$ are the variation of enthalpy and entropy of the adsorption process, respectively. A plot of $\Delta\boldsymbol{G}^{\circ}_{\boldsymbol{ads}}$ versus $\boldsymbol{T}$ gives a straight line with a slope of $-\Delta\boldsymbol{S}^{\circ}_{\text{ads}}$ and an intercept of $\Delta\boldsymbol{H}^{\circ}_{\text{ads}}$. The calculated values of $\Delta\boldsymbol{H}^{\circ}_{\text{ads}}$ and $\Delta\boldsymbol{S}^{\circ}_{\boldsymbol{ads}}$ are 28.5 kJmol^{-1} and 0.2 kJmol^{-1}K^{-1}. The positive sign of $\Delta\boldsymbol{H}^{\circ}_{\boldsymbol{ads}}$ reveals that the adsorption of inhibitor molecules is an endothermic process and the negative value suggests exothermic adsorption. Generally, an exothermic adsorption process suggests either physisorption or chemisorption while endothermic process is attributed to chemisorption[37]. The values of $\Delta\boldsymbol{S}^{\circ}_{\boldsymbol{ads}}$ in the presence of acid red are large and positive, meaning that an increasing in disordering takes place in going from reactants to the metal-adsorbed species reaction complex[52,53]. Also entropy $\Delta\boldsymbol{S}^{\circ}_{\text{ads}}$ and the enthalpy $\Delta\boldsymbol{H}^{\circ}_{\text{ads}}$ of adsorption can be calculated from the following integrated van't Hoff equation[51]:

Table 6 — Equilibrium adsorption parameters for acid red on steel surface in 1 M HCl solution.

Temperature K	$\boldsymbol{K}_{\boldsymbol{ads}}$ L mol^{-1}	$\Delta\boldsymbol{G}^{\circ}_{\text{ads}}$ kJ mol^{-1}
298	5.03×10^{3}	-31.1
318	1.93×10^{4}	-36.7
338	1.97×10^{4}	-39.1

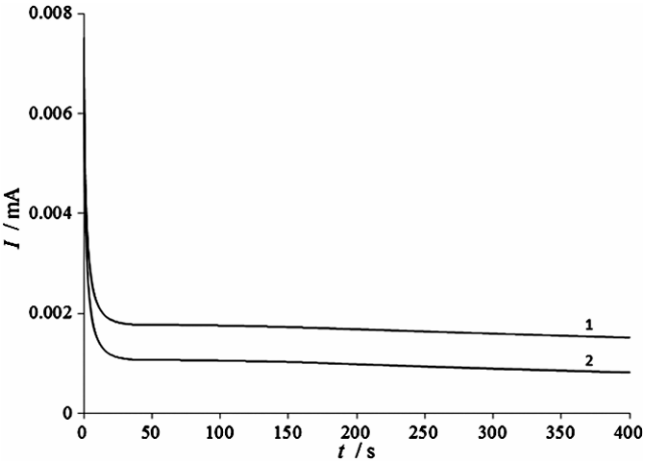

Fig. 6 — Current transients of steel electrode at -0.4 V: (1) Blank, (2) 100 ppm of acid red

.

$$\ln K_{ads} = -\frac{\Delta H^{\circ}_{ads}}{RT} + \frac{\Delta S^{\circ}_{ads}}{R} + \ln\frac{1}{55.5} \qquad ...(11)$$

The plots of $\ln K_{ads}$ versus T^{-1} represent a slope of ($-\Delta H°_{ads}/R$) and intercept of [$-\ln(55.5)+\Delta S°_{ads}/R$] for adsorption of acid red on steel surface. The calculated values of $\Delta H°_{ads}$ and $\Delta S°_{ads}$ are 28.66 kJmol^{-1} and 0.2 kJ mol^{-1} K^{-1}. It can be seen that the value of enthalpy of adsorption in Gibbs-Helmholtz equation agrees with the one obtained using van't Hoff equation.

Chronoamperometry

In order to gain more insight about the effect of inhibitor on the electrochemical behavior of steel in 1 M HCl solution, potentiostatic current-time transients were recorded. Fig. 6 shows the current transients of steel electrode at -0.4 V vs. Ag/AgCl applied anodic potential. Initially the current decreases monotonically with time. The decrease in the current density is due to the formation of corrosion products layer on the anode surface and reach a steady state value. In presence of the inhibitor lower dissolution and steady state current was obtained and electrode was inhibited from corrosion due to inhibitor adsorption.

Surface analysis

In order to further confirm the corrosion inhibition ability of inhibitor, SEM analyses was applied. After specimen immersion in acid solution without inhibitor for 6 h, the resulting morphology is shown in Fig. 7a. The micrograph is typical of a corroded surface appeared to dissolve uniformly with deep terraces. Fig. 7b shows the micrographs of steel after

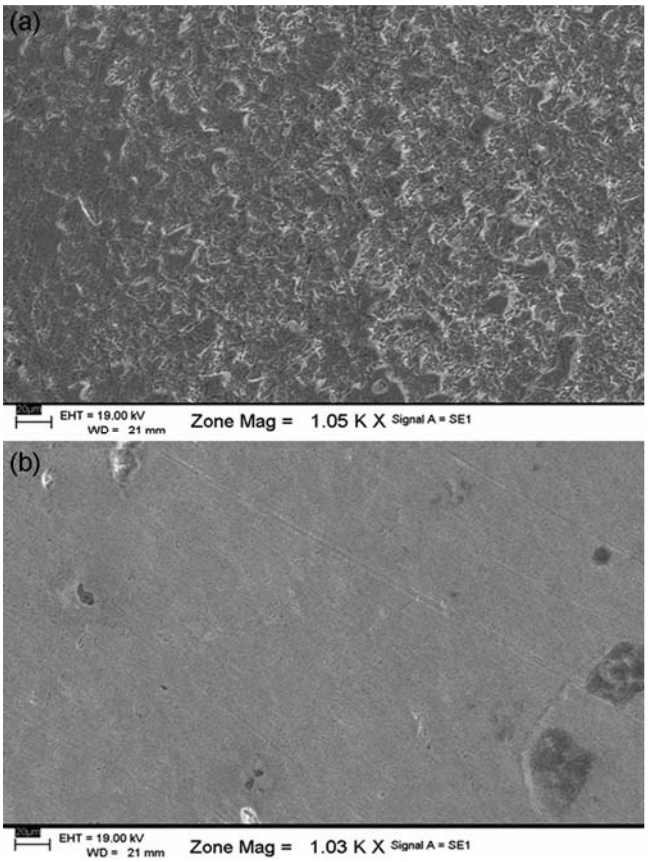

Fig. 7 — SEM micrograph of steel surface after immersion in free acid solution in (a) 1 M HCl (b) 100 ppm of acid red.

immersion in acidic solutions containing 100 ppm acid red. As can be seen from these figures, it is obvious that the surface looks more uniform and becomes more flat in the presence of inhibitor. It is observed that, inhibitor provided good protection film on the steel surface. This is in good agreement with the result obtained from the EIS tests that in presence of inhibitor in solution increase the exponent ***n*** of the double layer capacitance.

Conclusion

Acid red has a considerable inhibition effect on steel corrosion in 1 M HCl solution. Inhibition efficiency of this compound increases with increasing their concentrations due to the formation of a film on the steel surface.

Corrosion current density is increased by increasing the temperature, but the increasing rate in lower in the presence of acid red.

The potentiodynamic polarization curves indicate that these compounds inhibit both cathodic hydrogen

evolution reactions and anodic metal dissolution. So behave as mixed type corrosion inhibitors.

Impedance measurements indicate that with increasing inhibitor concentration, the polarization resistance increases, while the double layer capacitance decreases.

The adsorption of this compound on the steel surface obeys the Langmuir adsorption isotherm.The thermodynamic adsorption parameters show that the inhibitor is absorbed by a spontaneous endothermic process and chemisorptions process can be suggested for this compound.

Surface studies show that the surface of sample in solution with inhibitor molecules looks more flat and more uniform with lower roughness than that in the uninhibited solution.

References

1 Singh S K, Mukherjee A K & Singh M M, ***Indian J Chem Technol***, 18 (2011) 291.
2 Sharma M & Singh G, ***Indian J Chem Technol***, 18 (2011) 351.
3 Niknejad Khomami M, Danaee I, Attar A A & Peykari M, ***Trans Indian Inst Met***, 65 (2012) 303.
4 Gogoi P K & Barhai B, ***Indian J Chem Technol***, 17 (2010) 291.
5 Danaee I, Ghasemi O, Rashed G R, Rashvand Avei M & Maddahy M H, ***J Mol Struct***, 1035 (2013) 247.
6 Singh S K, Mukherjee Ashim K & Singh M M, ***Indian J Chem Technol***, 15 (2008) 174.
7 Jafari H, Danaee I, Eskandari H & Rashvand Avei M, ***Ind Eng Chem Res***, 52 (2013) 6617.
8 Ghasemi O, Danaee I, Rashed G R, Rashvand Avei M & Maddahy M H, ***J Mater Eng Perform***, 22 (2013) 1054.
9 Joseph B, John S, Aravindakshan K K & Joseph A, ***Indian J Chem Technol***, 17 (2010) 425.
10 Toliwal S D, Jadav K & Pavagadhi T, ***Indian J Chem Technol***, 18 (2011) 301.
11 Sharma M, Chawla J & Singh G, ***Indian J Chem Technol***, 16 (2009) 339.
12 Tebbji K, Aouniti A, Attayibat A, Hammouti B, Oudda H, Benkaddour M, Radi S & Nahle A, ***Indian J Chem Technol***, 18 (2011) 244.
13 Deng S, Li X & Fu H, ***Corros Sci***, 53 (2011) 3596.
14 Sathiyabama J, Rajendran S, Selvi J A & Amalraj A J, ***Indian J Chem Technol***, 15 (2008) 462.
15 Deng S, Li X & Fu H, ***Corros Sci***, 53 (2011) 760.
16 Li X, Deng S & Fu H, ***Corros Sci,*** 52 (2010) 3413.
17 Bultel H & Vogt J B, ***Procedia Eng***, 2 (2010) 917.
18 Danaee I, Niknejad Khomami M & Attar A A, ***J Mater Sci Technol***, 29 (2013) 89.
19 Macdonald J R, ***Solid State Ion***, 13 (1984) 147.
20 Danaee I, ***J Electroanal Chem***, 662 (2011) 415.
21 John S & Joseph A, ***Indian J Chem Technol***, 17 (2010) 176.
22 Yadav M, Yadav P N & Sharma U, ***Indian J Chem Technol***, 20 (2013) 363.
23 Migahed M A, Abd-El-Raouf M, Al-Sabagh A M & Abd-El-Bary H M, ***Electrochim Acta***, 50 (2005) 4683.
24 Migahed M A, Nassar I F, ***Electrochim Acta***, 53 (2008) 2877.
25 Popova A, Christov M, Raicheva S & Sokolova E, ***Corros Sci***, 46 (2004) 1333.
26 Ghasemi O, Danaee I, Rashed G R, Rashvand Avei M & Maddahy M H, ***J Cent South Univ***, 20 (2013) 301.
27 Amar H, Tounsi A, Makayssi A, Derja A, Benzakour J & Outzourhit A, ***Corros Sci***, 49 (2007) 2936.
28 Kumar H & Chaudhary R S, ***Indian J Chem Technol***, 17 (2010) 181.
29 Emregul K C & Atakol O, ***Mater Chem Phys***, 82 (2003) 188.
30 Rosliza R, Nik W B & Senin H B, ***Mater Chem Phys***, 107 (2008) 281.
31 Abdel-Gaber A M, Abd-El-Nabey B A, Sidahmed I M, El-Zayady A M & Saadawy M, ***Corros Sci***, 48 (2006) 2765.
32 Danaee I & Noori S, ***Int J Hydrogen Energy***, 36 (2011) 12102.
33 Gunasekaran G, Chauhan L R, ***Electrochim Acta***, 49 (2004) 4387.
34 Danaee I, Niknejad Khomami M & Attar A A, ***Mater Chem Phys***, 135 (2012) 658.
35 Ramesh Kumar S, Danaee I, Rashvand Avei M & Vijayan M, ***J Mol Liq***, 212 (2015) 168.
36 Chaieb E, Bouyanzer A, Hammouti B & Benkaddour M, ***Appl Surf Sci***, 246 (2005) 199.
37 Martinez S & Stern I, ***Appl Surf Sci***, 199 (2002) 83.
38 Avci G, ***Colloid Surf A Physicochem Eng Aspects***, 317 (2008) 730.
39 Begum A S, Mallika J & Gayathri P, ***E-J Chem***, 7 (2010) 185.
40 Szauer T & Brand A, ***Electrochim Acta***, 26 (1981) 1219.
41 DanaeeI, Gholami M, Rashvand Avei M & Maddahy M H, ***J Ind Eng Chem***, 26 (81.
42 Joseph B, John S, Joseph A & Narayana B, ***Indian J Chem Technol***, 17 (2010) 366.
43 Herrag L, Hammouti B, Elkadiri S, Aouniti A, Jama C, Vezin H & Bentiss F, ***Corros Sci***, 52 (2010) 3042.
44 Gholami M, Danaee I, Maddahy M H & Rashvandavei M, ***Ind Eng Chem Res***, 52 (2013) 14875.
45 Ahamad I, Prasad R & Quraishi M A, ***Corros Sci***, 52 (2010) 933.
46 Haldar N, Shukla H S & Udayabhanu, G, ***Indian J Chem Technol***, 19 (2012) 173.
47 Hoseinzadeh A R, Danaee I & Maddahy M H, ***J Mater Sci Technol***, 29 (2013) 884.
48 Cardoso S P, Reis F A, Massapust F C, Costa J F, Tebaldi L S, Araújo L F L, Silva M V A, Oliveira T S, Gomes J A C P & Hollauer E, ***Quim Nova***, 28 (2005)756.
49 Karimi A, Danaee I, Eskandari H & Rashvan Avei M, ***Prot Met Phys Chem Surf***, 51 (2015) 899.
50 Ebenso E E & Obot I B, ***Int J Electrochem Sci***, 5 (2010) 2012.
51 Hoseinzadeh A R, Danaee I & Maddahy M H, ***Z Phys Chem***, 227 (2013) 403.
52 Bentiss F, Lebrini M & Lagrenee M, ***Corros Sci***, 47 (2005) 2915.
53 Noor E A & Al-Moubaraki A H, ***Int J Electrochem Sci***, 3 (2008) 806.